2013 IREP Symposium-Bulk Power System Dynamics and Control –IX (IREP), August 25-30, 2013, Rethymnon, Greece

Further Investigations on a Phasor Measurement-Based Algorithm Utilized for Voltage Instability Awareness

Glauco N. Taranto Carlos Oyarce
Federal University of Rio de Janeiro / COPPE
Brazil

Sandro Corsi
Consultant
Italy

Abstract

This paper further investigates the strengths and weaknesses of the algorithm first proposed in [1]. The algorithm estimates the Thevenin-equivalent parameters from an EHV bus. As a tutorial, the paper assesses the performance of the algorithm applied to a very simple electric circuit. The performance of the algorithm is compared to a recursive least square algorithm with noisy measurements. At the end, the algorithm is applied to a long-term voltage instability scenario and to a marginally stable scenario in the Nordic32 benchmark system.

I. Introduction

Along with the popularization of the phasor measurement units (PMU), the use of Thevenin equivalents for long-term voltage instability identification has been acknowledged by many researchers in the last 14 years [1-5]. A few ideas for the determination of the Thevenin parameters have been proposed in those references. References [2-4] utilize the recursive least square (RLS) algorithm, whereas [5] utilizes the Tellegen's theorem. Corsi & Taranto [1] proposed an algorithm that is based on electric circuit theory and on a predict-and-correct procedure. The Corsi-Taranto (CT) algorithm is not explained in this paper. Interested readers should refer to [1].

This paper further investigates the strengths and weaknesses of the CT algorithm. The algorithm is applied to estimate the equivalent Thevenin parameters (voltage and impedance) "seen" from a load bus [2], as represented by the simple electric circuit shown in Fig.1. Based on local measurements of the voltage and current phasors at the load bus, it is possible to estimate the Thevenin parameters. The Thevenin impedance is compared to the load impedance (computed with the same measurements) and the maximum power transfer (MPT) approaching is inferred.

The paper is organized as follows: Section II presents, as a tutorial, the performance of the CT algorithm for changes in the impedance and in the source voltage magnitude for the circuit shown in Fig.1, and it also shows the performance of the CT algorithm for increasing values of the Thevenin resistance. Section III presents a comparative analysis between the CT and RLS algorithms with varying levels of noise in the measurements. Section IV presents the performance of the CT algorithm in long-term unstable and marginally stable scenarios artificially created in the Nordic32 benchmark test system [6]. Some concluding remarks are made in Section V.

II. Tutorial Tests

In order to assess the correctness and performance of the CT algorithm, it is presented, as a tutorial, some simulation results in the simple electric circuit shown in Fig.1.

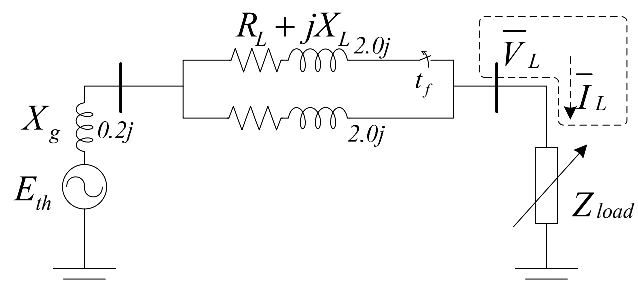

Fig.1 – Simple electric circuit to assess the performance of the CT algorithm

The following experiments were performed:

1. Variation of the circuit impedance by the opening of switch t_f;
2. Variation of the source voltage E_{th} with a 10% increase. The voltage changes from 1.0 to 1.1 pu;
3. Variation of the resistance R_L for values ranging from zero ohm to 10% of X_L.

All the simulations performed in this section consider a variation of the load impedance (Z_{load}) according to the curve given in Fig.2. The considered load impedance curve guarantees that the circuit is not "at rest" at any instant of the analysis period.

978-1-4799-0199-9/13/$31.00 ©2013 IEEE

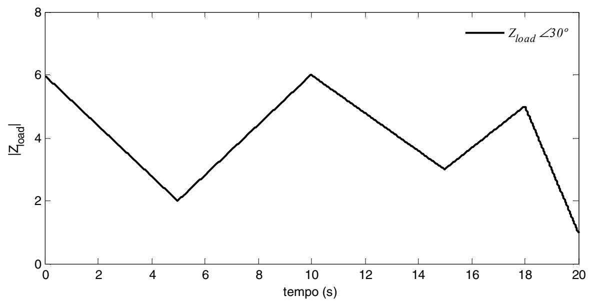

Fig.2 – Time variation of the load impedance magnitude

The CT algorithm uses the voltage and current phasors (V_L and I_L), as indicated in Fig.1, to estimate the Thevenin parameters, which in this case are known. The characteristics of the simple circuit are as follows: the voltage source is represented as a constant voltage E_{th} = 1.0 pu behind a constant reactance X_g = j0.2. The transmission lines (TL) are initially represented only by constant series reactances X_L = j2.0 each. The series resistance R_L will be considered nonzero in Section II.3. The line charging is neglected and load is represented as constant impedance (Z_{load}) with a lagging power factor (pf = cos 30^o). All computations consider a sampling rate of 50 Hz, i.e., voltage and current phasors are acquired every 20 ms. The identification is supposed to be real time unless during initialization and right after slope changes.

II.1. Variation of the Circuit Impedance

Both TLs are initially in service, and the first experiment consists of opening the switch t_f at 10 s, to assess the performance of the CT algorithm in estimating the Thevenin impedance (which is actually a reactance in this case). Figure 3 shows the performance of the algorithm in estimating the Thevenin reactance before the line opening, which is equal to j1.2 pu, and after the line opening that becomes j2.2 pu.

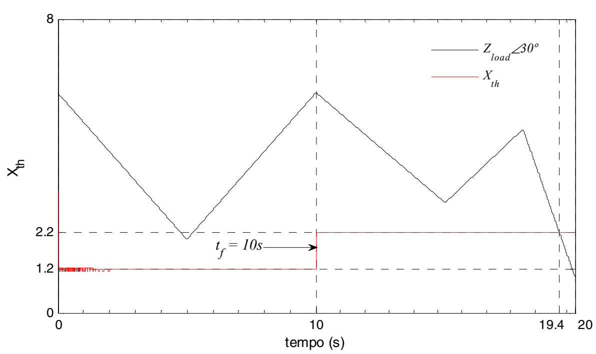

Fig.3 – Estimated Thevenin reactance (red) and imposed load impedance magnitude (black)

Figure 4 shows a zoomed in view of the estimated Thevenin reactance. The larger initial variation is due to the characteristic of the CT algorithm in the initialization process (readers should refer to [1]). Once the correct value is reached the algorithm presents minor variations of the estimated parameter, which is around 1%. Figure 4(c) shows the estimated source voltage magnitude (*Eth*). As expected the identified source voltage magnitude does not vary at 10 s.

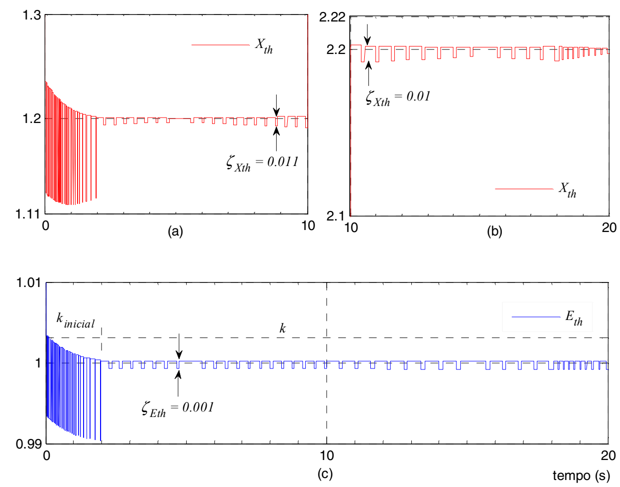

Fig.4 – Performance of the algorihtm in estimating the Thevenin reactance. (a) with both TLs in service; (b) with only one TL in service. (c) Estimated source voltage magnitude.

A closer look at Fig.4 clearly shows how the algorithm works. When the estimation is above the true value of the parameter being estimated, the algorithm forces a reduction in the estimation, or vice-versa. Figure 4 also shows the absolute value of the steady-state error of the algorithm (approx. 1%) which must exist to enforce the predict-and-correct principle of the CT algorithm.

II.2. Variation of the Source Voltage

The second experiment consists in changing the source voltage magnitude originally from 1.0 pu to 1.1 pu at 10 s. In this experiment both lossless TLs are in service.

Figure 5 shows the identified equivalent reactance and source voltage magnitude. It can be noticed that the equivalent reactance has a transient variation around 10 s, but swiftly recovers to the correct value of j1.2 pu. Figure 6 highlights the fast convergence of the algorithm when the source voltage increases 10%. After approximately half second the correct value is identified. It corresponds to an iterative computation of 25 subsequent samples of the current and voltage phasors.

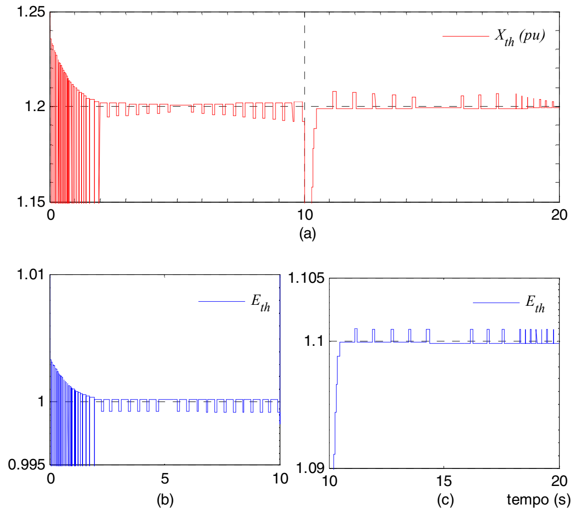

Fig.5 – Performance of the algorihtm in estimating the Thevenin source voltage magnitude. (a) estimated equivalent reactance; (b) estimated source voltage magnitude before 10s; (c) estimated source voltage magnitude after 10s.

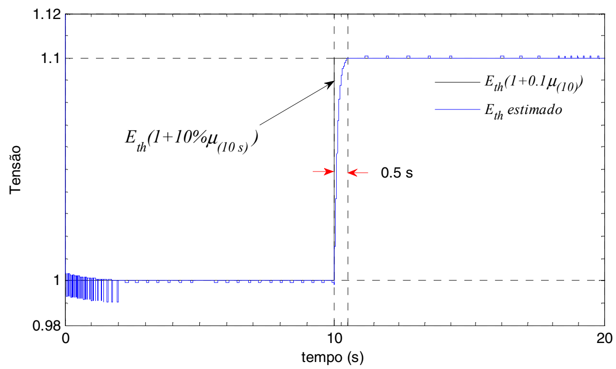

Fig.6 – Performance of the algorihtm in estimating the Thevenin source voltage magnitude.

II.3.Sensitivity Analysis with Respect to Thevenin Resistance

One fundamental assumption made by the CT algorithm [1] was neglecting the resistive part of the Thevenin-equivalent impedance. This assumption confines the application of the CT algorithm in EHV buses, where the ratio R/X is small (< 0.1). How adequate is the application of the CT algorithm in systems with large R/X ratio, will be tackled in the sequel.

This section presents a sensitivity analysis with respect to the resistance (R_L) of the circuit given in Fig.1, with both TLs in service. Defining $R_{th} = R_T/2$, Table 1 presents the values of the resistances to be considered in the analysis, as a percentage of the TL reactance (X_L).

Table 1 – Considered Thevenin Resistances

Percentage	$R_L(pu)$	$R_{th}(pu)$
$0.0\%X_L$	0.00	0.000
$2.5\%X_L$	0.05	0.025
$5.0\%X_L$	0.10	0.050
$7.5\%X_L$	0.15	0.075
$10\%X_L$	0.20	0.100

Figure 7 shows the performance of the algorithm in identifying the Thevenin impedance for the values of R_L defined in Table 1.

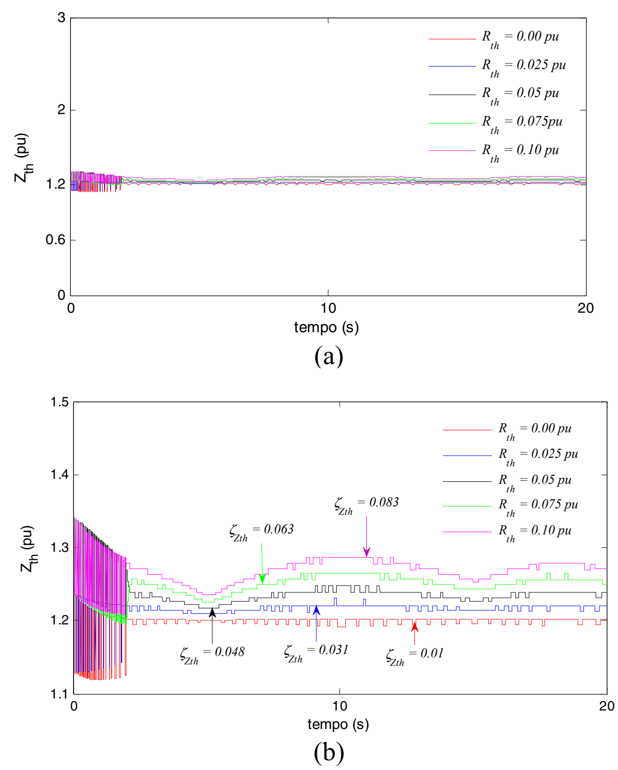

Fig.7 – (a) Performance of the CT algorithm to identify the Thevenin impedance as a function of the resistance; (b) Zoomed in view of the plots in (a).

In Fig.7(b) it is shown the maximum error obtained for each curve. The maximum error is defined as the maximum difference from the correct value of the Thevenin impedance. A lesser abrupt load changing will probably yield smaller errors, but errors will remain while there is resistance increasing (R_L).

The true impedance values for each corresponding resistances are:

$$\overline{Z}_{th(R_{th}=0.0)} = 0.0 + j1.2 = 1.2\angle 0^{\circ}$$

$$\overline{Z}_{th(R_{th}=0.025)} = 0.025 + j1.2 = 1.2003\angle 88.8^{\circ}$$

$$\overline{Z}_{th(R_{th}=0.05)} = 0.05 + j1.2 = 1.201\angle 87.6^{\circ}$$

$$\overline{Z}_{th(R_{th}=0.075)} = 0.075 + j1.2 = 1.2023\angle 86.4^{\circ}$$

$$\overline{Z}_{th(R_{th}=0.10)} = 0.1 + j1.2 = 1.2042\angle 85.2^{\circ}$$

The larger errors are:

$$\varsigma_{Zth(Rth=0)} = 1.2011\text{-}1.2001 = 0.01$$

$$\varsigma_{Zth(Rth=0.025)} = 1.2308\text{-}1.2003 = 0.031$$

$$\varsigma_{Zth(Rth=0.05)} = 1.2485\text{-}1.201 = 0.048$$

$$\varsigma_{Zth(Rth=0.075)} = 1.265\text{-}1.2023 = 0.063$$

$$\varsigma_{Zth(Rth=0.10)} = 1.2869\text{-}1.2042 = 0.083$$

The corresponding errors in percentages are:

$$\%\varsigma_{Zth(Rth=0)} = 0.01/1.2 = 0.83\%$$

$$\%\varsigma_{Zth(Rth=0.025)} = 0.031/1.2003 = 2.58\%$$

$$\%\varsigma_{Zth(Rth=0.05)} = 0.048/1.201 = 3.99\%$$

$$\%\varsigma_{Zth(Rth=0.075)} = 0.063/1.2023 = 5.24\%$$

$$\%\varsigma_{Zth(Rth=0.10)} = 0.083/1.2042 = 6.89\%$$

The sensitivity analysis is summarized in Table 2, which also presents the maximum errors obtained in the source voltage (E_{th}) identification. Figure 8 shows the performance of the CT algorithm in identifying the source voltage as a function of the resistance.

Table 2 – Considered Thevenin Resistances

Error (%)		E_{th}	Z_{th}
R_L	R_{th}		
$R_L = 0.0\% X_L$	$R_{th} \approx 0.0\% X_{th}$	0.1%	0.83%
$R_L = 0.5\% X_L$	$R_{th} \approx 2.5\% X_{th}$	0.3%	2.58%
$R_L = 5.0\% X_L$	$R_{th} \approx 5.0\% X_{th}$	0.62%	3.99%
$R_L = 7.5\% X_L$	$R_{th} \approx 7.5\% X_{th}$	0.95%	5.24%
$R_L = 10\% X_L$	$R_{th} \approx 10\% X_{th}$	1.24%	6.89%

The algorithm had a better performance in identifying the source voltage than in identifying the equivalent impedance. As expected, the errors increase as the ratio R/X becomes larger.

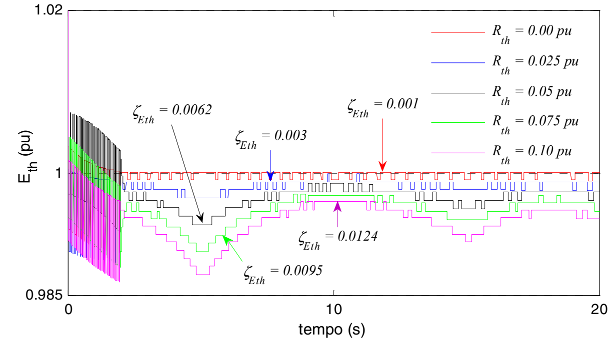

Fig.8 – Performance of the CT algorithm to identify the Thevenin source voltage as a function of the resistance.

III. Performance of the Algorithm with Noisy Measurements – A Comparative Analysis

This section presents a comparative analysis between the CT algorithm and the RLS method used in [3] in the presence of a system dynamic model and noise in the voltage and current phasor measurements.

The comparative analysis of the algorithms is made with time-domain simulations performed in a small test system proposed in [7]. Figure 9 shows the one-line diagram of the test system taken from [7]. Conventional electromechanical fundamental-frequency models are utilized for the electrical components. The generator is equipped with a summing-type soft-limiting OEL model [7]. The transformers connected between Buses #4 and #5 are equipped with on-load tap changers, where the first tap movement has a delay of 30 s, and the subsequent tap changes have a delay of 5 s. Real-life typical parameters for the generator, transformer and transmission lines are considered in the analysis.

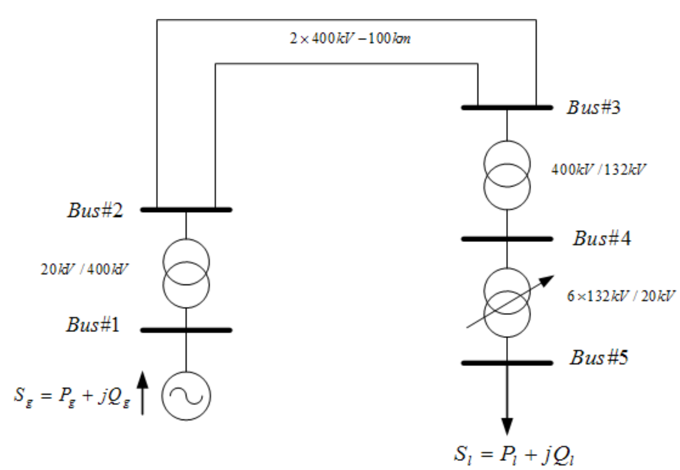

Fig.9 – One-Line Diagram of the Test System

The simulations consisted of a ramp increase in the system load connected in Bus #5 up to the point where the time-domain simulation software "crashed". Since the load is represented by an exponential model with voltage-dependent power consumption, the maximum loadability point (MLP) can be reached.

White noise is artificially added to the voltage and current phasors measured at Bus #3. The first attempt was done with a signal-to-noise ratio (SNR) equals do 90 dB. Figure 10 shows the Thevenin impedance identification with the RLS algorithm (blue plot) and with the CT algorithm (red plot). No filtering techniques are applied to either algorithm. Figure 10 also shows the load impedance curve (black plot). It can be noted that the CT algorithm has an inherit filtering characteristic not observed in the RLS algorithm. The high sensitivity of RLS at points of discontinuities (tap changes after 180 s) can be improved by means of averaging past information or by neglecting present information. Although effective, these techniques tend to delay the identification process.

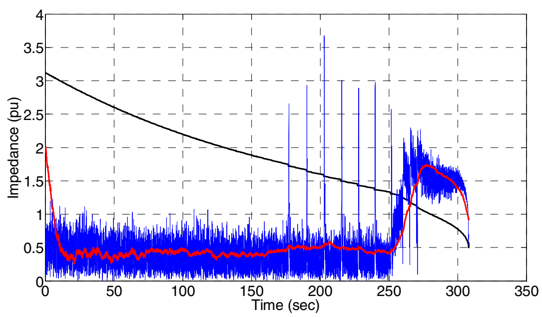

Fig.10 – Comparative performance of the CT vs RLS algorithms considering a SNR = 90 db and no filtering applied. (red – CT; blue – RLS)

Figure 11 shows the same simulation as depicted in Fig.10 with the impedance identified by RLS filtered by a moving average (MA) of 50 samples. The impedance identified by CT remains without any kind of filtering.

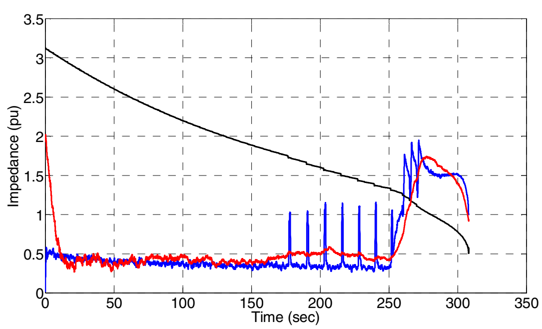

Fig.11 – Comparative performance of CT vs RLS (SNR = 90 dB) with a moving average filter applied in the RLS only. (red – CT; blue – RLS)

The second attempt was done with a SNR equals do 40 dB. Figure 12 shows the Thevenin impedance identification with the RLS algorithm (blue plot) and with the CT algorithm (red plot). The MA filter is applied in the RLS result, and no filtering technique is applied in the CT result. Although the performance of both algorithms degrades substantially, the CT algorithm is able to capture an increase tendency in the Thevenin impedance, whereas the RLS algorithm behaves insensitive along the whole simulation.

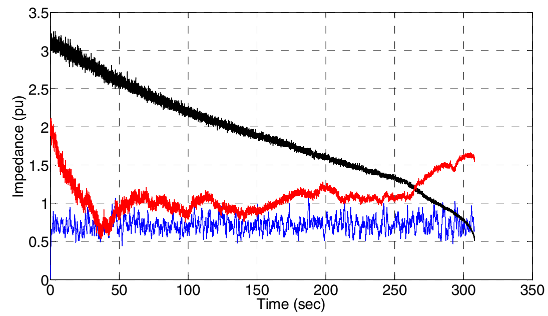

Fig.12 – Comparative performance of CT vs RLS (SNR = 40 dB) with a MA filter applied in the RLS. (red – CT; blue – RLS)

IV. Performance results in the Nordic32 System

This section presents the performance of the CT algorithm in detecting long-term voltage instability in the Nordic32 test system [6]. The Nordic32 test system is one of the two test systems that are being proposed by the IEEE Working Group on test systems for voltage stability analysis. The system scenario is a high transfer condition from the generating area (North) to the heavily loaded area (Central), according to Fig.13. A three-phase short-circuit followed by the opening of the transmission line connecting Bus #4032 to Bus #4044 (marked with two red X in Fig.13) in the North-Central corridor leads the short-term-stable operating condition to long-term voltage instability. The long-term instability is caused by the actuation of the closed-loop controls of the OLTCs and OELs modeled in the system.

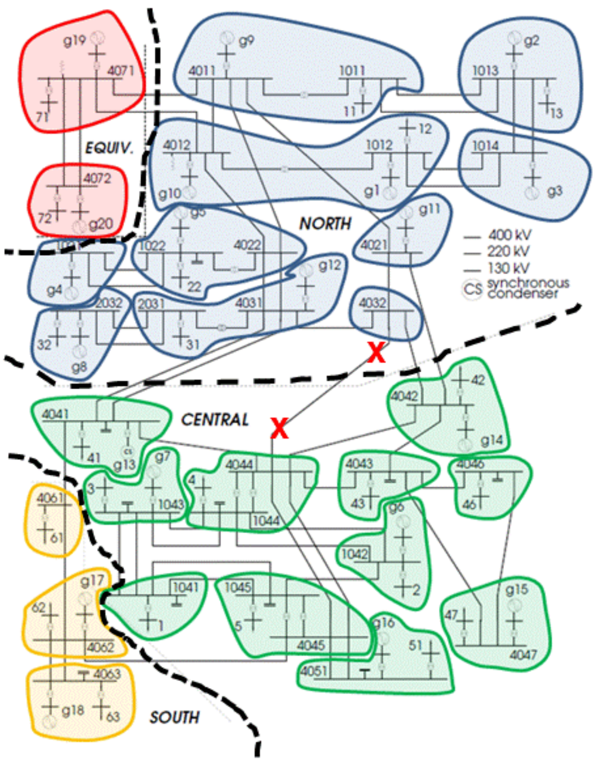

Fig.13 – Nordic32 Benchmark System

Figure 14 shows the tap position of 6 OLTCs located in the Central Area. Figure 15 highlights the tap position of the OLTC 1041 together with its primary voltage at Bus #1041, and its regulated secondary voltage at Bus #1041-1.

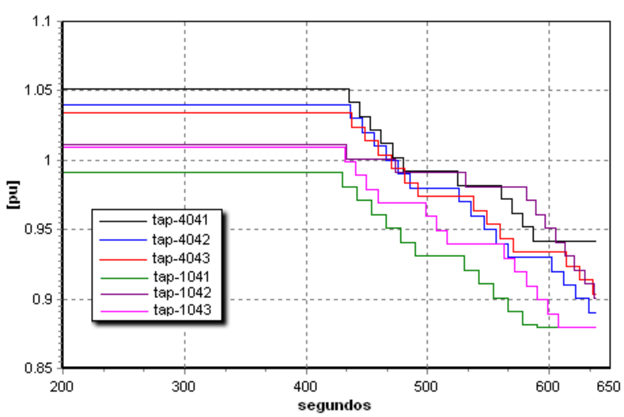

Fig.14 – Tap position of 6 OLTCs

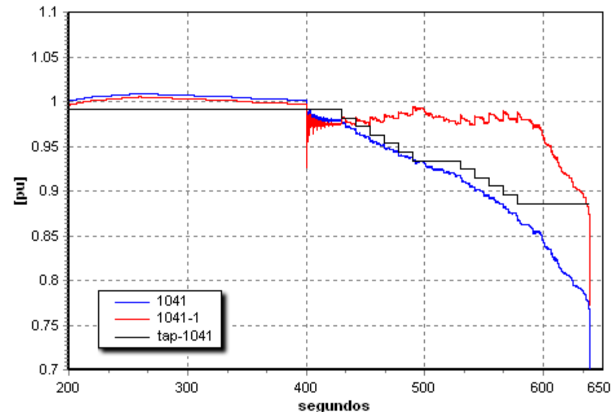

Fig.15 – Tap position (black) of OLTC 1041 and primary (blue) and regulated secondary (red) voltage magnitudes.

Figure 16 shows the field current of one generator in the North Area (G12) and five generators in the Central Area (G6, G7, G14, G15, G16). It can be noted that the OEL model allows time-constrained overloads.

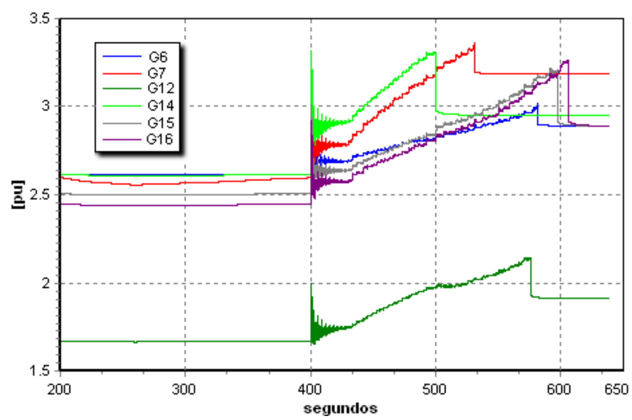

Fig.16 – Field current of 6 generators

In Fig.17 it is shown the terminal voltages of generators G2, G4, G7 and G14. Generators G2 and G4 are located in the North Area and G7 and G14 are located in the Central Area. The plots clearly show the moments when the field currents of G14 and G7 are forced to their steady-state limits around 500 s and 540 s, respectively. From those moments on, the generators loose voltage control and the terminal voltages sharply degrade. Generators G2 and G4, located far from the heavy-load area, maintain terminal voltage control along the whole simulation.

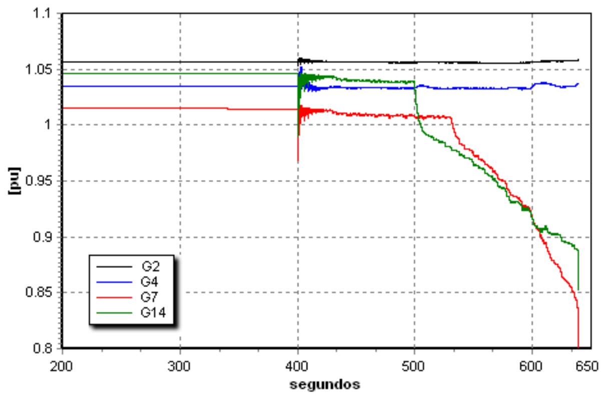

Fig.17 – Terminal voltage magnitudes of 4 generators

Figure 18 shows the voltage magnitudes of five load buses in the Central Area. It can be noted that the system is short-term angle stable since the electromechanical oscillations are damped out from 400 s to around 430 s.

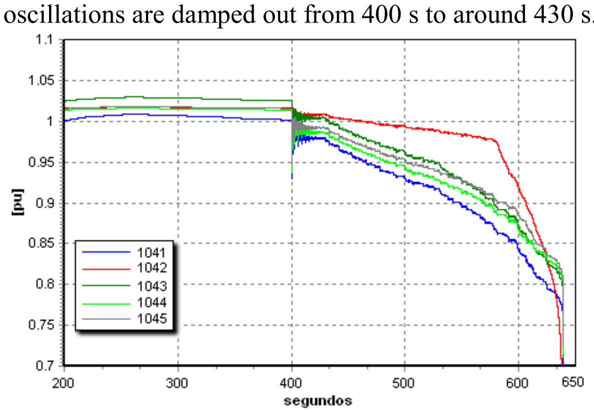

Fig.18 – Voltage magnitudes of 5 load buses in the Central Area

IV.1. Performance of the CT Algorithm for an Unstable Case

Figure 19 shows the Thevenin and the load impedance of the load bus #1041 for the long-term unstable case previously presented in Figs.14-18.

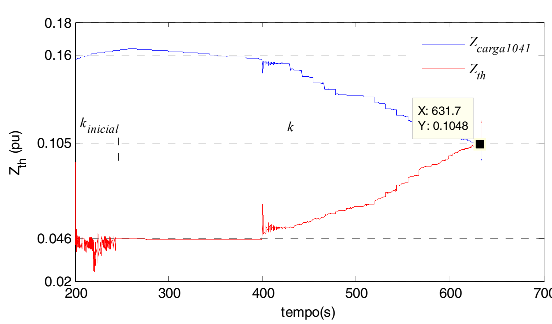

Fig.19 – Thevenin (red) and load (blue) impedances for the Nordic32 system – unstable case.

IV.2. Performance of the CT Algorithm for a Marginally Stable Case

The performance of the CT algorithm is also assessed in a situation where the system remains marginally stable. Figure 20 shows the Thevenin impedance (red plot) and the load impedance (blue plot) "seen" from Bus #1041 for the marginally stable case. It can be noted that the long-term equilibrium point is reached at around 750 s. It is also interesting to remark that the long-term equilibrium point is reached after the MLP for Bus#1041. This can happen because of the voltage-dependent load models that are being considered in the simulations.

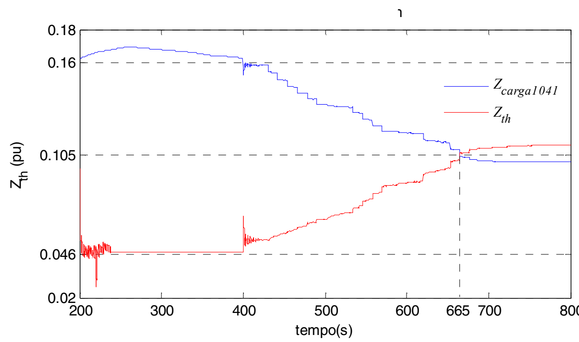

Fig.20 – Thevenin (red) and load (blue) impedances for the Nordic32 system – marginally stable case.

V. Conclusions

The paper confirms the reliability and repeatability of the CT identification results obtained in previous works [1, 8]. The method computes the real-time Thevenin's equivalent impedance "seen" from a given load bus by simply using the local voltage and current fast phasor measurements.

Tutorial results obtained with a simple electric circuit show the predict-and-correct characteristic of the CT algorithm, its correctness and its fast convergence to the Thevenin parameters identification.

The CT algorithm is less sensitive to measurements with noise when compared to the RLS algorithm.

The quality of the identification result is confirmed when considering a mid-size power system described by comprehensive electromechanical dynamic models.

The CT algorithm conceived for EHV grid applications shows lower quality identification results while increasing the equivalent impedance ratio between the resistance and the reactance values. Notwithstanding, this ratio has to increase considerably before determining a significant error in the objective of voltage instability identification. Therefore, the CT algorithm strength is high while minor is its weakness.

References

[1] S. Corsi & G. N. Taranto, "A Real-Time Voltage Instability Identification Algorithm Based on Local Phasor Measurements," *IEEE Transactions on Power Systems*, vol. 23, no. 3, pp. 1271-1279, August 2008.

[2] K. Vu, M. M. Begovic, D. Novosel, and M. M. Saha, "Use of Local Measurements to Estimate Voltage-Stability Margin," *IEEE Transactions on Power Systems*, vol. 14, no. 3, pp. 1029–1035, August 1999.

[3] B. Milosevic and M. Begovic, "Voltage-Stability Protection and Control Using a Wide-Area Network of Phasor Measurements," *IEEE Transactions on Power Systems*, vol. 18, no. 1, pp. 121–127, February 2003.

[4] M. Zima, M. Larsson, P. Korba, C. Rehtanz and G. Andersson, "Design Aspects for Wide-Area Monitoring and Control Systems," *Proceedings of the IEEE*, Vol. 93, No. 5, pp. 980-996, May 2005.

[5] I. Smon, G. Verbic and F. Gubina, "Local Voltage-Stability Index Using Tellegen's Theorem", *IEEE Transactions on Power Systems*, Vol. 21, No. 3, pp. 1267-1275, August 2006.

[6] T. Van Cutsem, "Description, Modelling and Simulation Results of a Test System for Voltage Stability Analysis", *IEEE WG on Test Systems for Voltage Stability Analysis*, Document Version 2, November 2010.

[7] S. Corsi & G. N. Taranto, "Voltage Stability – the Different Shapes of the "Nose"," *Proceedings of the Bulk Power Systems Dynamics and Control VII*, IREP Symposium, Charleston, USA, August 2007.

[8] S. Corsi & G. N. Taranto, "Reliability Analysis of Voltage Instability Risk Indicator Based on a Phasor-Data Real-Time Identification Algorithm", *European Transactions on Electrical Power*, Vol. 21, No. 4, pp. 1610-1628, May 2011.